JOURNAL OF AIRCRAFT
Vol. 41, No. 1, January–February 2004

In-Flight Weight and Balance Identification Using Neural Networks

Moshe Idan,* Gil Iosilevskii,† and Sergey Nazarov‡
Technion—Israel Institute of Technology, 32000 Haifa, Israel

Weight and longitudinal center-of-gravity position of an aircraft are valuable information for flight monitoring, automatic flight control, and fault detection and identification algorithms. In trimmed symmetric flight (as cruise, climb, or descent) the aircraft weight is counteracted mainly by the aerodynamic lift, whereas the associated couple is counterbalanced by a moment generated by an appropriate elevator deflection. Because, for given flight conditions, the aerodynamic lift and pitching moment are functions of the angle of attack and elevator deflection only, the last two variables carry the information about the aircraft weight and its longitudinal center-of-gravity position. It is demonstrated that this information can be effectively recovered in flight using nonparametric artificial neural networks (NNs), pretrained on flight-test data. To enhance the accuracy and speed up the training process, basic flight mechanics relations are incorporated into the NN. It is also demonstrated that the NN-based lift and pitching moment functions can be used a posteriori to estimate the aircraft longitudinal neutral point.

Introduction

WEIGHT and longitudinal location of the center of gravity (to be referred to as weight and balance or W&B in the sequel) greatly affect the static and dynamic characteristics of an aircraft, and therefore are desirable information for automatic flight control, fault detection and identification systems, and other onboard functions. They are also desirable for in-flight monitoring by the pilot. W&B identification for a commercial aircraft is the subject matter of this exposition.

In most known applications only the total takeoff weight of an aircraft is determined on the ground and then roughly updated during flight based on the change in the fuel quantity.[1,2] The latter is obtained either by a direct measurement or estimated based on measured fuel consumption. This can lead to erroneous weight and balance data caused by inaccuracy in the takeoff weight and difficulties associated with fuel quantity/consumption measurements.

Aircraft weight and its center-of-gravity (c.g.) position vary relatively slowly compared to other flight variables. Therefore, W&B identification scheme can be based on force and moment balance during trimmed phases of flight only, where the governing equations are expected to be the simplest. In fact, in trimmed symmetric flight (as cruise, climb, or descent) the weight of an aircraft is counteracted mainly by the aerodynamic lift, whereas the associated couple is counterbalanced by a pitching moment caused by an appropriate elevator deflection. Because for given Mach and altitude the aerodynamic lift and pitching moment are functions of the angle of attack and elevator deflection only, the last two variables carry the information about the aircraft weight and its longitudinal c.g. position. Thus, in principle, the W&B data can be recovered in flight from readily measured flight variables, provided that an accurate, yet simple, aerodynamics model of the aircraft is available to the onboard computer.

Because of aerodynamic interactions between lifting surfaces, local flow separations and local shock formations, a sufficiently accurate aerodynamic model of even ordinary looking aircraft is quite complex, and usually lacks analytical description. Nonetheless, it is suggested that an aerodynamics-based nonparametric W&B estimator can be effectively constructed using artificial neural networks (NNs), which are known for their capability to approximate any smooth function to within a required accuracy.[3] An additional benefit of using NNs in the present context is the availability of rapid training procedures and numerical tools.[4]

The paper is organized as follows. The methodology of in-flight estimation of the aircraft weight and longitudinal location of its c.g. is presented in the next section. It is followed by a short review of the main features of NNs as model approximators and by a description of the specific NN structure used in this study. The data sets used for training and evaluation of the NN are addressed next, succeeded by a discussion of the pertinent results. The paper is concluded by a few remarks and summary.

Methodology

Frequency Separation

The current work is aimed mainly at W&B identification for civil aircraft applications, although it can equally be applicable for other flight vehicles. For civil aircraft most of the flight is performed along straight paths, with relatively short periods of heading and airspeed changes. Accordingly, W&B identification can be restricted to trimmed (steady), symmetric phases of flight, where flaps, slats, and landing gears are retracted. There is no conceptual difficulty to extend the analysis to different flight phases with different configurations, but their short duration makes such an extension ineffective.

Unlike most of the flight variables, weight and c.g. location of an aircraft change very slowly compared to the characteristic timescales of the aircraft dynamics. Accordingly, even if the flight takes place in unsteady atmosphere, aircraft dynamic response to air disturbances can be entirely ignored, and steady-state analysis of trimmed flight can be used to a full effect.

Basic Relations of Trimmed Flight

In a steady symmetric flight aerodynamic lift L, drag D, and propulsion T forces offset the gravity force W, whereas the total pitch couple M_y on the airplane vanishes. Before explicitly stating these equilibrium conditions, it will prove convenient to introduce standard dimensionless quantities, where the product of dynamic pressure q and wing area S is used as a unit of force, and the wing mean aerodynamic chord c is used as a unit of length. In particular, the dimensionless total pitch couple C_M and gravity force C_W are

Received 27 January 2003; revision received 14 May 2003; accepted for publication 14 May 2003.

*Senior Lecturer, Faculty of Aerospace Engineering. Associate Fellow AIAA.
†Senior Lecturer, Faculty of Aerospace Engineering.
‡Research Associate, Faculty of Aerospace Engineering.

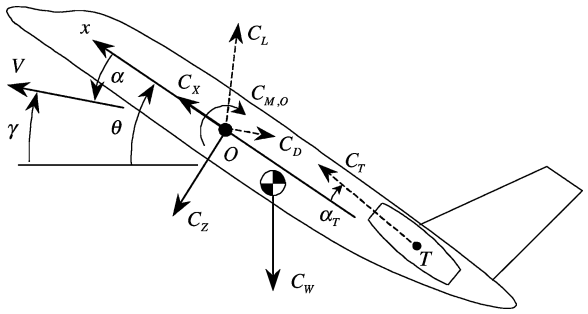

Fig. 1 Nondimensional forces and moments: - - - - > , forces involved in Eqs. (5) and (6); and ——>, forces and moments involved in Eqs. (3), (4), and (7).

defined by

$$C_M = M_y/qSc \tag{1}$$

$$C_W = W/qS \tag{2}$$

and, similarly, the dimensionless lift, drag, and propulsion forces. Following common notation, the dimensionless forces will be occasionally referred to as "coefficients."

The following analysis will be carried out in a reference frame commonly used in flight mechanics, with x axis pointing forward, y axis pointing into the right wing, and z axis pointing down. The origin O of this reference frame can be chosen freely. The triple (x, y, z) will denote the (dimensionless) coordinates of a point relative to this system. The dimensionless forces and moments, as well as the reference frame, are depicted schematically in Fig. 1.

The equilibrium conditions involve two equations of force balance and one of pitching-moment balance. The two conditions for the force balance take on the form

$$C_X - C_W \sin\theta = 0 \tag{3}$$

$$C_Z + C_W \cos\theta = 0 \tag{4}$$

where

$$C_X = C_L \sin\alpha - C_D \cos\alpha + C_T \cos\alpha_T \tag{5}$$

and

$$C_Z = -(C_L \cos\alpha + C_D \sin\alpha + C_T \sin\alpha_T) \tag{6}$$

are the components of the combined aerodynamic and propulsion forces along the respective axes, whereas α, θ, and α_T are the angle of attack, the pitch-attitude angle, and the thrust inclination angle.

With subscripts cg and T referring to the aircraft c.g. and engine locations in the reference frame, the condition of vanishing pitching moment takes on the form

$$C_{M,O} + C_Z x_{\text{cg}} - C_X z_{\text{cg}} = 0 \tag{7}$$

where

$$C_{M,O} = C^a_{M,O} + C_T x_T \sin\alpha_T + C_T z_T \cos\alpha_T \tag{8}$$

is the sum of the aerodynamic pitching moment $C^a_{M,O}$ and the moment produced by the thrust about the reference point O. Using Eqs. (3) and (4), Eq. (7) can be recast as

$$C_{M,O} + C_Z(x_{\text{cg}} + z_{\text{cg}} \tan\theta) = 0 \tag{9}$$

The lift, drag, and aerodynamic pitch-moment coefficients are functions of Mach number M, angle of attack α, and elevator deflection δ_e only. Were these functions known, then, given M, α, δ_e, θ, z_{cg}, and α_T, Eqs. (3), (4), and (9) could have been solved for the weight and thrust coefficients and for longitudinal c.g. position x_{cg}. In particular, with $\gamma = \theta - \alpha$ being the flight-path angle,

$$C_W = \frac{C_D \sin(\alpha + \alpha_T) + C_L \cos(\alpha + \alpha_T)}{\cos(\theta + \alpha_T)} \tag{10}$$

$$C_T = \frac{C_D \cos\gamma + C_L \sin\gamma}{\cos(\theta + \alpha_T)} \tag{11}$$

$$x_{\text{cg}} = -\left(\frac{C_{M,O}}{C_Z} + z_{\text{cg}} \tan\theta\right) \tag{12}$$

Implementation

The main drawback of the analytical scheme just presented is that the complex functions describing the aerodynamic coefficients are, in general, not known. These functions can be estimated using preliminary design tools, computed numerically using computational-fluid-dynamics codes, estimated from wind-tunnel data, or estimated from flight-test data. Of these, the last option seems to be the most practical for in-flight W&B identification purposes.

Separation between thrust and drag from flight-test data is, in general, not possible without additional information concerning either of the two forces. Hence, we would like to alter the formulation so that no distinction between thrust and drag will be needed. This implies reducing the number of dependent variables to weight and longitudinal c.g. position only (no thrust), and, consequently, reducing the number of independent equations.

Referring to Eqs. (4) and (9), we note that C_Z supplemented by pitch attitude contains all of the information about the weight coefficient, whereas a combination of C_Z and $C_{M,O}$ contains all of the information about the longitudinal c.g. position. In other words, models for C_Z and $C_{M,O}$ should suffice for W&B identification. Both coefficients involve thrust, and hence are functions of both the aerodynamic variables (M, α, δ_e) and the flight-path angle γ [see Eqs. (6), (8), and (11)].

Flight-test data are invariably contaminated by measurement noise. To obtain an accurate W&B identification, this noise has to be filtered or smoothed out. This rules out the construction of a W&B identification algorithm based on interpolation between flight-test points. Instead, it is suggested that artificial NNs can be effectively used to create a smooth map relating the coefficients C_Z and $C_{M,O}$ to $(M, \alpha, \delta_e, \gamma)$ or, ultimately, the weight and c.g. position to $(M, \alpha, \delta_e, \gamma)$ and dynamic pressure q.

Neural Networks

General

Thus, our goal is to generate a smooth nonparametric map that will relate the various flight variables to the aircraft weight and c.g. location. This map, which is mainly governed by the aerodynamic characteristics of the aircraft, should be constructed from limited data measured in flight tests. In this work we propose using NNs for this task. NNs were chosen for two main reasons. First, multiple-layer NNs are known to be universal nonparametric appoximators of smooth functions, that is, in principle, for any given smooth function, a NN can be found to approximate it to any accuracy.[3,5,6] Second, a modular structure of a NN provides a multitude of efficient training algorithms for computing the NN parameters so as to best fit the training set.[4,7]

NNs have been successfully utilized in a large variety of applications (e.g., see, Refs. 4 and 7 for sample lists). Noteworthy is their recent application to weight identification of a helicopter in hover flight.[8] Although it addressed only a limited flight regime, it clearly showed that NN can be trained on noisy flight-test data and then used for weight identification in flight.

Structured NN

An attempt to use standard multiple-layer feed-forward NN architecture, with and dynamic pressure q as inputs and W and x_{cg} as outputs resulted in NNs with a large number of neurons, excessive

training time, and poor convergence. To overcome this difficulty, we suggest embedding the basic flight mechanics relations (2), (4), and (12) into a fixed nontraining part of the NN structure. Once these relations need not to be approximated by training elements, the sought overall functional relations can be reconstructed with fewer neurons, and therefore fewer NN parameters. This has a favorable effect on both the training process and the over fitting tendency of the NNs, especially when training the NN on noisy flight-test data.

Following Eqs. (2), (4), and (12),

$$W = -qSC_Z/\cos\theta \tag{13}$$

$$x_{\mathrm{cg}} = -C_M/C_Z \tag{14}$$

where

$$C_M = C_{M,O} + C_Z z_{\mathrm{cg}} \tan\theta \tag{15}$$

Here, both C_Z and C_M are functions of $(M, \alpha, \delta_e, \gamma)$; C_M is also a function of z_{cg}. Throughout this exposition we shall assume that z_{cg} is fixed (for a commercial jet, variations of z_{cg} during flight are expected to be small). Hence, NN can be designed so as to (implicitly) identify the dimensionless coefficients C_Z and C_M, with W and x_{cg} computed by prescribed (not trained) relations of Eqs. (13) and (14). This is depicted schematically in Fig. 2, which clearly identifies the adaptive (trained) and prescribed (not trained) portions of the NN. This architecture, designated as WXNN in the sequel, provides satisfactory performance. It will serve as the basis for the following refinement.

Weight identification based on Eq. (13) depends only on C_Z and can be performed independently of c.g. identification per Eq. (14), which depends also on C_M. This allows replacing the WXNN by two separate NNs: WNN, which identifies the weight, and XNN, which, supplemented by WNN, identifies the c.g. location. This architecture is shown in Fig. 3. A noticeable advantage of the two-part NN is in the sequencing of the training procedure: instead of training the entire WXNN en bloc, WNN is trained first, and then used "frozen" to provide an additional input for training the XNN. The sequencing

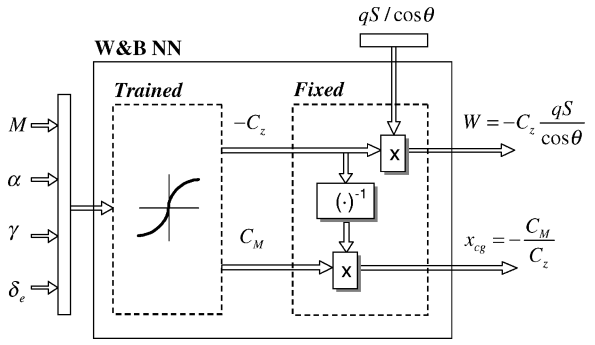

Fig. 2 One-part NN architecture WXNN.

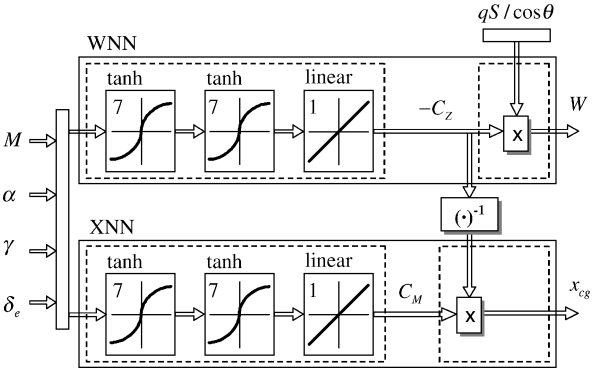

Fig. 3 Two-part NN architecture.

of the training process shortens the training time, whereas the decoupling between the WNN and XNN affects favorably the weight estimation accuracy.

The effect of NN architecture on estimation accuracy can be concluded from the difference in the training processes of the two-output WXNN and the single-output WNN. Training of the latter entails adjusting the parameters (or weights) of the NN so as to minimize the mean-square error between the NN output and the training data, that is, the aircraft weight. For multioutput NNs, such as WXNN, the NN weights are adjusted so as to minimize a weighted mean-square error of the outputs, prescribed by the relative importance of the NN outputs. Thus, in the two-output WXNN the aircraft weight identification accuracy is invariably compromised against that of the c.g., and therefore it is expected to be less accurate than a comparably sized single-output WNN.

In principle, the last fixed layer of both WNN and XNN could have been omitted, with resulting NNs identifying C_Z and C_M instead of W and x_{cg}. However, NNs trained to minimize the mean-square estimation error in the coefficients should, in general, yield nonminimal estimation errors in W and x_{cg}. Specifically, a given error in C_Z yields variable, dynamic-pressure-dependent, error in weight identification. Similarly, a given error in C_M yields variable, C_Z-dependent, error in x_{cg}. Thus, the last layer of WNN and XNN provides an effective condition-dependent weighting to their respective outputs. It is worth noting that, albeit not optimally fitted, the coefficients C_Z and C_M can still be picked up as the outputs of the training portions of the respective NNs. This feature of the NNs will be utilized for identification of the aircraft longitudinal neutral point.

Training and Evaluation Data Sets

The proposed W&B identification concept has been tested on numerically simulated flight-test data of a transonic twin-engine 40,000-lb class commercial jet. The aircraft model has been derived within a project sponsored by the commission of the European communities[9]; it has been loosely based on the geometry, aerodynamic, and propulsion data of a typical business jet.[10] The aerodynamic data have been derived from real wind-tunnel measurements and hence included realistic interactions between surfaces, flow-separation effects, and local shock formations. Irregular behavior of the aerodynamic coefficients, especially at high angles of attack and transonic Mach numbers, ruled out analytical modeling, and they have been defined by interpolating functions (look-up tables).

The flight envelope of the aircraft is depicted in Fig. 4. It covers all possible combinations of flaps, slats, and aircraft weights. In this study the W&B identification has been limited to trimmed flight with no flaps, slats, and landing gears, away from stall regions. The

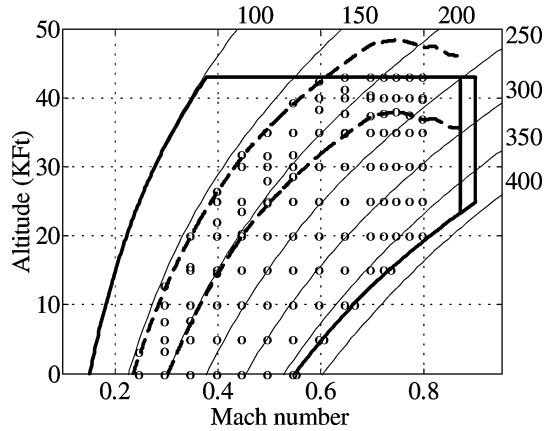

Fig. 4 Flight envelope and training data points: ——, the boundaries of the flight envelope; – – –, maximum lift coefficient for empty (top line) and maximum weights; ——, constant calibrated airspeed (in knots) curves; and ○, data points.

dashed lines mark the boundaries imposed by these limits on the flight envelope.

The particular aircraft used in this study featured sharp variations in all aerodynamic coefficients at and above Mach 0.8. Accordingly, two sets of NNs have been trained: one corresponding to Mach numbers below 0.8 and one for Mach numbers between 0.8 and 0.87. Because there is no conceptual difference between the two sets of NNs and in order to concentrate on the main issues of the NN training, evaluation, and postprocessing, the presentation will be limited to the NNs that have been trained for Mach numbers below 0.8.

To generate numerical "flight-test" data for the NN training, the aircraft was trimmed for a set of weights, longitudinal c.g. positions, Mach numbers, altitudes, and throttle settings. A trimming routine computed the respective angles of attack, pitch attitudes, elevator deflections, flight-path angles, and dynamic pressures. The Mach numbers have been regularly spaced between stall and maximum dynamic pressure limit or Mach 0.8 (whichever smaller); the altitudes ranged from sea level to stall limit or 43 Kft (whichever smaller). For each combination of Mach and altitude, there have been four weights and four c.g. positions, regularly spaced between their respective maximum and minimum values, and three throttle settings: idle, maximum, and the one corresponding to level flight. The respective minimal and maximal W and x_{cg} values are 26,000 and 43,000 lb and 19 and 40% of the mean aerodynamic cord (MAC).

All this resulted in 120 combinations of Mach and altitude at which the aircraft was trimmed; they are depicted in Fig. 4 together with lift coefficient and dynamic pressure limits. At each combination of Mach and altitude, there are up to 48 viable combinations of weight, c.g., and throttle settings, resulting in about 4000 test points altogether. It is believed that this number of test points, albeit high, is not entirely unreal for actual flight tests.

Real flight-test data are invariably noisy, with errors affecting all measured variables. For the sake of simplicity, all of the measurement errors have been replaced by equivalent errors in weight and c.g. position. For the training set these errors, shown in Fig. 5, have been chosen as white, zero-mean, Gaussian sequences, with standard deviations of 300 lb and 1.5% MAC, respectively.

The evaluation data set was constructed similarly to the training set, but was two orders of magnitude larger and contained over 350,000 test points of clean, noise-free data. In this set the Mach numbers have been regularly distributed between stall and maximum dynamic pressure or Mach 0.8 (whichever lower) every 0.01, whereas altitudes have been regularly distributed between sea-level and 43 Kft every 2.5 Kft, yielding about 700 flight conditions. At each of these conditions, there have been up to 1400 combinations of weight, c.g., and throttle settings, spanning the admissible range of those variables.

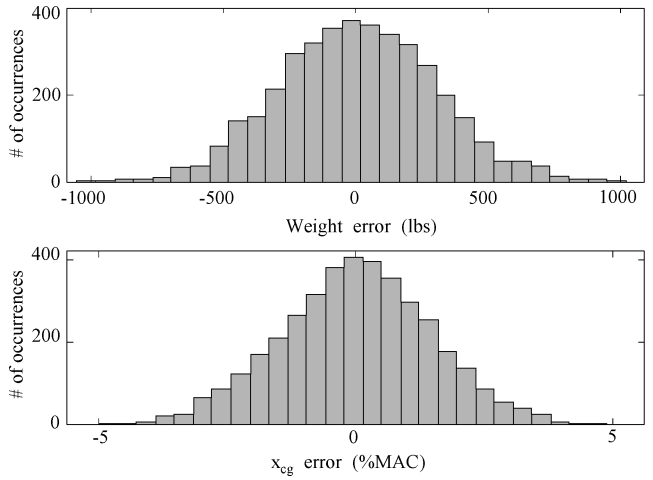

Fig. 5 Distributions of the measurement noise in the training data.

Results

NN Training

The W&B identification NNs presented in Fig. 3 were trained using the numerically generated noisy trimmed flight data, discussed before. The first task was to determine the structure of the training parts of the NNs, that is, determine the number of layers and the number and type of neurons in each layer. After several iterations the structures depicted in Fig. 3 were obtained, where both WNN and XNN have an identical layout of three hidden layers (MATLAB® terminology.[4]) Each of the first two layers has seven hyperbolic tangent sigmoid transfer functions, whereas the third layer is linear.

The two NNs were trained sequentially using Levenberg–Marquardt backpropagation and mean-squared error performance index.[4] Becaue of the noisy data, the training convergence goal was set to approximately the mean-squared value of the measurement noise. The distributions of the NN estimation errors while using the training data set are depicted in Fig. 6. They closely resemble the distributions of respective noises shown in Fig. 5, indicating that the NNs have effectively smoothed out the noisy training data and did not overfit it.

Evaluation Results

The trained NNs have been evaluated using the evaluation data-set presented earlier. Maximum absolute weight and longitudinal c.g. position estimation errors at each Mach/altitude combination are color coded in Figs. 7 and 8, respectively. Identification accuracy of 450 lb in weight and 1.6% MAC in c.g. position can be clearly seen.

The preceding presentation is probably somewhat conservative, showing only the extreme errors. A better insight can be gained from

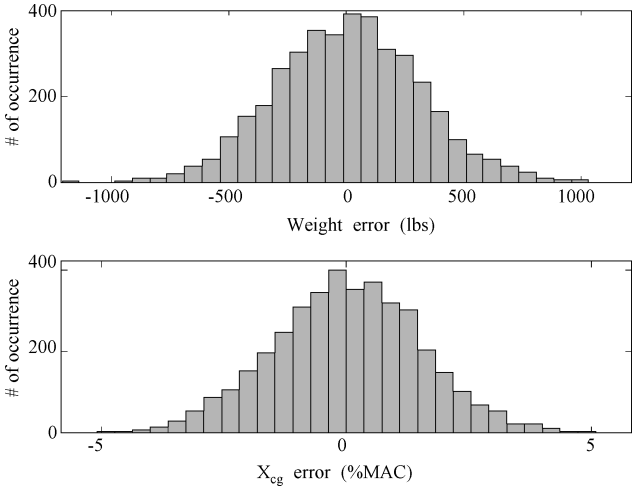

Fig. 6 Distributions of the NN estimation errors on the training data.

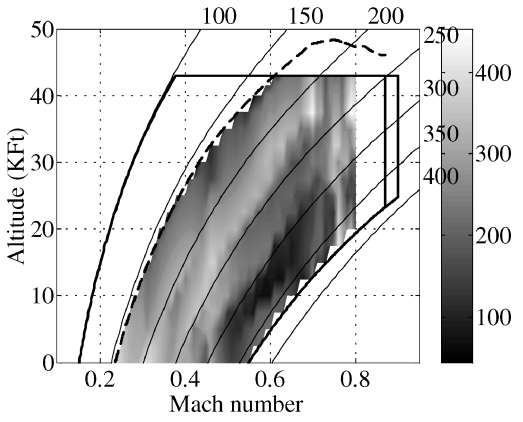

Fig. 7 WNN performance—maximum weight error, evaluation data set.

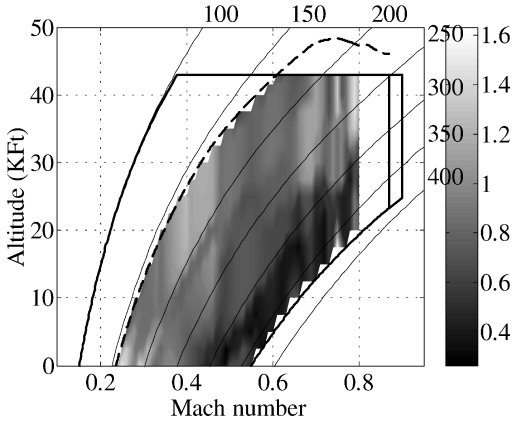

Fig. 8 XNN performance—maximum x_{cg} error, evaluation data set.

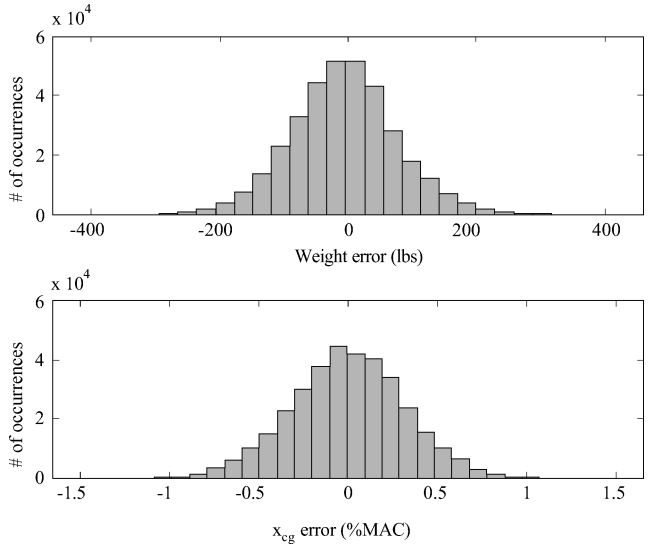

Fig. 9 NN performance—distribution of the estimation errors, evaluation data set.

the distribution of those errors, depicted in Fig. 9. It was verified that in 99% of the tested points the weight and the c.g. position have been identified with an accuracy better than 260 lb and 1% MAC, respectively. The former is roughly equivalent to a single (big) passenger, whereas the latter is equivalent to a c.g. shift when this passenger moves from one end of the aircraft to the other. These accuracies are expected to be satisfactory for most applications.

Postprocessing Capabilities—Neutral-Point Identification

Background

Longitudinal neutral point is, by definition, a point (x_n, z_n) along the aircraft where pitching moment is independent of the angle of attack. The location of this point is fundamental both in stability analysis of an aircraft and in its dynamic characteristics. We would like to demonstrate how x_n can be extracted from the W&B identification NNs.

Following Eq. (14), neutral-point location is given by[11]

$$x_n = -\frac{(\partial C_M/\partial\alpha)_{M,\delta_e,C_T}}{(\partial C_Z/\partial\alpha)_{M,\delta_e,C_T}} \tag{16}$$

It is essential that the differentiation in Eq. (16) be performed while keeping M, δ_e, and C_T constant, as indicated explicitly by the respective subscripts.

The W&B identification paradigm is based on the estimation of C_Z and C_M, as given by Eqs. (13) and (14). These coefficients are only implicit in the W&B identification algorithm, but they can be obtained as the outputs of the third layer of the respective NNs (see Fig. 3). Hence it seems plausible that the neutral-point location can be estimated by manipulating the internal signals of the NNs. The major complication of such an implementation is that in the NNs the coefficients C_Z and C_M are functions of M, α, δ_e, and γ, and not of M, α, δ_e, and C_T; constant C_T does not imply constant γ. On the contrary, in trimmed flight a change in α, with M, δ_e, and C_T kept constant, will result in a change in γ.

A detailed derivation of the longitudinal neutral point location x_n based on signals available in the W&B NNs is presented in the Appendix. A practical approximation of x_n is given by

$$x_n \approx -\frac{(\partial C_M/\partial\alpha)_{M,\delta_e,\gamma}}{(\partial C_Z/\partial\alpha)_{M,\delta_e,\gamma}} + \frac{1}{C_Z}\left(\frac{\partial C_M}{\partial\gamma}\right)_{M,\alpha,\delta_e}\left(\gamma - 2\frac{C_Z}{\pi Ae}\right) \tag{17}$$

where A is the aspect ratio of the wing and e is a semi-empirical coefficient, which can be estimated from the knowledge of the wing's planform. For the particular aircraft used for this study, it was approximated by 0.6 ± 0.1 (Ref. 12).

Numerical Differentiation and Results

The actual neutral point of the aircraft has been computed using Eq. (16), by numerically differentiating the aircraft aerodynamic model. This model was provided in a form of look-up tables, with points separated 1 deg α apart; accordingly, all derivatives have been computed using central differences with 1-deg step. This computation, although approximate, served as a reference for evaluation of NN performance.

Since the W&B identification NNs, constructed from neurons with smooth transfer functions, have closed-form analytical derivatives, all of the partial derivatives in Eq. (17) can, in principle, be computed analytically. However, using analytically computed derivatives, Eq. (17) yielded unsatisfactory results compared to the reference. At the same time using central differences with 1-deg step—as in the reference computation—yielded reasonable identification accuracies of about 5% MAC in neutral-point location for 99% of the cases tested while using the evaluation data set. These results are shown in Figs. 10 and 11.

The preceding behavior is rooted in the numerical characteristics of the aerodynamic model used in this study. As already noted,

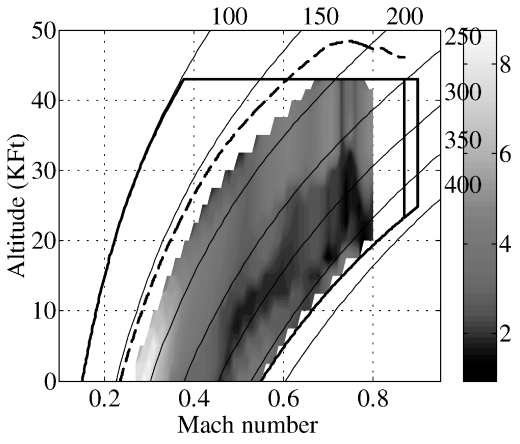

Fig. 10 Maximum errors of NN-based neutral-point estimation.

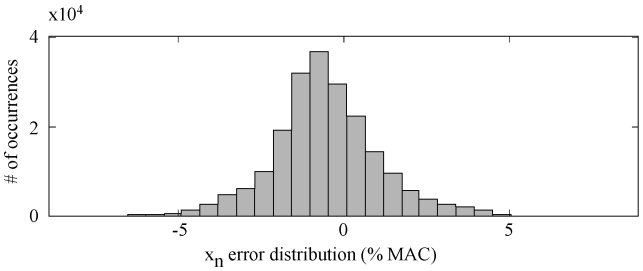

Fig. 11 Distribution of the NN-based neutral-point estimation error.

the latter has been based on wind-tunnel measurements, separated 1 deg apart. The points of the training and evaluation sets have been constructed using linear interpolation between database points. Accordingly, the aerodynamic model, and thus the trim data on which the NNs have been trained, has discontinuous first derivatives with respect to angle of attack and the elevator deflection. Because of the continuous nature of the NN elements, these discontinuities are smoothed by WNN and XNN; still there is an inherent difference between large and small step differentiations of the NNs.

Summary

A structured neural-network-based algorithm for in-flight estimation of the aircraft weight and longitudinal location of its c.g. has been presented. The network has been trained on a limited set of numerically generated flight-test data. Good identification accuracy has been demonstrated over the entire flight envelope of a small civil commercial aircraft. It was shown that the particular neural-network architecture chosen could be also used to estimate the aircraft longitudinal neutral-point position. Such in-flight weight and balance identification system is an invaluable tool for many onboard functions such as automatic flight-control system, fault detection and identification algorithms, flight-path planning, and more.

Appendix: Derivation of Eq. (16)

Longitudinal neutral-point location is given by Eq. (16), namely,

$$x_n = -\frac{(\partial C_M/\partial\alpha)_{M,\delta_e,C_T}}{(\partial C_Z/\partial\alpha)_{M,\delta_e,C_T}} \tag{A1}$$

The derivatives involved in this equation are the subject matter of this Appendix.

Given C_Z and C_M as functions of M, α, δ_e, and γ, their derivatives with respect to α, with M, δ_e, and C_T kept constant, are

$$\left(\frac{\partial C_Z}{\partial\alpha}\right)_{M,\delta_e,C_T} = \left(\frac{\partial C_Z}{\partial\alpha}\right)_{M,\delta_e,\gamma} + \left(\frac{\partial C_Z}{\partial\gamma}\right)_{M,\alpha,\delta_e}\left(\frac{\partial\gamma}{\partial\alpha}\right)_{M,\delta_e,C_T} \tag{A2}$$

$$\left(\frac{\partial C_M}{\partial\alpha}\right)_{M,\delta_e,C_T} = \left(\frac{\partial C_M}{\partial\alpha}\right)_{M,\delta_e,\gamma} + \left(\frac{\partial C_M}{\partial\gamma}\right)_{M,\alpha,\delta_e}\left(\frac{\partial\gamma}{\partial\alpha}\right)_{M,\delta_e,C_T} \tag{A3}$$

The first two terms on the right-hand side of either Eq. (A2) or Eq. (A3) can be computed by direct differentiation (either analytical or numerical) of the respective NNs and therefore require no particular attention. The derivative $\partial\gamma/\partial\alpha$ is addressed next.

Multiplying Eqs. (3) and (4) by $\cos\alpha$ and $\sin\alpha$, respectively, and adding the two yields the well-known formula

$$\sin\gamma = [C_T\cos(\alpha+\alpha_T) - C_D]/C_W \tag{A4}$$

for the flight-path angle. Using Eq. (4) again, Eq. (A4) can be recast as

$$\frac{C_D\cos\theta - C_Z\sin\gamma}{\cos\theta\cos(\alpha+\alpha_T)} = C_T \tag{A5}$$

Equation (A5) can now be differentiated with respect to α, which, together with Eq. (A2), can be manipulated so as to obtain

$$\left(\frac{\partial\gamma}{\partial\alpha}\right)_{M,\delta_e,C_T} = -\left\{\frac{\partial}{\partial\alpha}\left[\frac{C_Z\sin\gamma}{\cos\theta\cos(\alpha+\alpha_T)}\right]_{M,\delta_e,\gamma} - \frac{\partial}{\partial\alpha}\left[\frac{C_D}{\cos(\alpha+\alpha_T)}\right]_{M,\delta_e}\right\} \Bigg/ \frac{\partial}{\partial\gamma}\left[\frac{C_Z\sin\gamma}{\cos\theta\cos(\alpha+\alpha_T)}\right]_{M,\alpha,\delta_e} \tag{A6}$$

For commercial transonic jets with flaps, slats, and landing gears retracted, all angles, as well as C_D to C_L ratio, are small quantities. Accordingly, the last equation can be approximated, to a very good accuracy, by

$$\left(\frac{\partial\gamma}{\partial\alpha}\right)_{M,\delta_e,C_T} \approx -\frac{\gamma(\partial C_Z/\partial\alpha)_{M,\delta_e,\gamma} - (\partial C_D/\partial\alpha)_{M,\delta_e}}{C_Z + \gamma(\partial C_Z/\partial\gamma)_{M,\alpha,\delta_e}} \tag{A7}$$

From Eqs. (6) and (11) it follows that

$$C_Z = -C_L\left[\cos\alpha + \frac{\sin\gamma\sin\alpha_T}{\cos(\theta+\alpha_T)}\right] - C_D\left[\sin\alpha + \frac{\cos\gamma\sin\alpha_T}{\cos(\theta+\alpha_T)}\right] \tag{A8}$$

whence

$$\left(\frac{\partial C_Z}{\partial\gamma}\right)_{M,\alpha,\delta_e} = -C_L\sin\alpha_T\frac{\cos(\alpha+\alpha_T)}{\cos^2(\theta+\alpha_T)} - C_D\sin\alpha_T\frac{\sin(\alpha+\alpha_T)}{\cos^2(\theta+\alpha_T)} \approx C_Z\alpha_T \tag{A9}$$

This estimate suggests that the second term of the denominator in Eq. (A7) is negligible, in which case,

$$\left(\frac{\partial\gamma}{\partial\alpha}\right)_{M,\delta_e,C_T} \approx -\frac{\gamma}{C_Z}\left(\frac{\partial C_Z}{\partial\alpha}\right)_{M,\delta_e,\gamma} + \frac{1}{C_Z}\left(\frac{\partial C_D}{\partial\alpha}\right)_{M,\delta_e} \tag{A10}$$

The first term on the right of Eq. (A10) is immediately available by direct differentiation of WNN. The second term is, in general, unknown, and hence is estimated based on preliminary design rules. To this end, it is assumed that the drag coefficient can be approximated by a parabolic polar of the form

$$C_D = C_{D,0} + KC_L^2 \tag{A11}$$

where $C_{D,0}$ and K are the parasite and the induced drag coefficients, respectively. The former of these is irrelevant to the course of the following derivations; the latter is commonly approximated by[12]

$$K \approx 1/\pi Ae \tag{A12}$$

where A is the aspect ratio of the wing (about 10 for commercial jets) and e is planform-dependent empirical coefficient (typically between 0.5 and 0.8).[12] Noting Eq. (A8), differentiation of Eq. (A11) implies

$$\left(\frac{\partial C_D}{\partial\alpha}\right)_{M,\delta_e} \approx 2KC_Z\left(\frac{\partial C_Z}{\partial\alpha}\right)_{M,\delta_e,\gamma} \tag{A13}$$

Because C_Z is of the order unity, this equation supports our assumption that the derivative of C_D with respect to angle of attack is small as compared with that of C_Z.

Using Eqs. (A9) and (A10), Eq. (A2) yields

$$\left(\frac{\partial C_Z}{\partial\alpha}\right)_{M,\delta_e,C_T} \approx (1-\alpha_T\gamma)\left(\frac{\partial C_Z}{\partial\alpha}\right)_{M,\delta_e,\gamma} + \alpha_T\left(\frac{\partial C_D}{\partial\alpha}\right)_{M,\delta_e} \approx \left(\frac{\partial C_Z}{\partial\alpha}\right)_{M,\delta_e,\gamma} \tag{A14}$$

the expression on the right stems the small angle and small drag-to-lift ratio assumptions. Similarly, using Eqs. (A9) and (A10) in Eq. (A3), and combining the result with Eq. (A14) into Eq. (A1) yields

$$x_n \approx -\frac{(\partial C_M/\partial\alpha)_{M,\delta_e,\gamma}}{(\partial C_Z/\partial\alpha)_{M,\delta_e,\gamma}} + \frac{1}{C_Z}\left(\frac{\partial C_M}{\partial\gamma}\right)_{M,\alpha,\delta_e}\left[\gamma - \frac{(\partial C_D/\partial\alpha)_{M,\delta_e}}{(\partial C_Z/\partial\alpha)_{M,\delta_e,\gamma}}\right] \tag{A15}$$

Because the derivatives of C_Z and C_M can be obtained by direct differentiation of the respective NNs, then, under the assumption in Eq. (A13), the neutral point is given by

$$x_n \approx -\frac{(\partial C_M/\partial\alpha)_{M,\delta_e,\gamma}}{(\partial C_Z/\partial\alpha)_{M,\delta_e,\gamma}} + \frac{1}{C_Z}\left(\frac{\partial C_M}{\partial\gamma}\right)_{M,\alpha,\delta_e}\left(\gamma - 2\frac{C_Z}{\pi Ae}\right) \tag{A16}$$

Equation (A16) is obviously approximate. To assess its accuracy, consider the second term on its right-hand side in more detail, focusing first on the derivative $\partial C_M/\partial\gamma$. With Eqs. (A5) and (15) Eq. (8) can be manipulated so as to obtain

$$\begin{aligned} C_M &= C^a_{M,O} + C_T(x_T\sin\alpha_T + z_T\cos\alpha_T) + C_Z z_n\tan\theta \\ &= C^a_{M,O} - \frac{C_Z\sin\gamma - C_D\cos\theta}{\cos\theta\cos(\alpha+\alpha_T)}(x_T\sin\alpha_T + z_T\cos\alpha_T) \\ &\quad + C_Z z_n\tan\theta \end{aligned} \tag{A17}$$

Noting Eq. (A9), the derivative of Eq. (A17) yields

$$\frac{1}{C_Z}\left(\frac{\partial C_M}{\partial\gamma}\right)_{M,\alpha,\delta_e} \approx (-x_T\alpha_T + z_n - z_T) \tag{A18}$$

which is the distance of the neutral point from the thrust axis. This distance is, in general, of order one (for the particular aircraft used for this study, it is about 0.6), whereas both γ and $2C_Z/(\pi Ae)$ are of order 0.1. Hence, the entire second term in Eq. (A16) might turn out to be of the order of 0.1. This is a nonnegligible quantity. Nonetheless, it suggests that a typical 20% relative error in e might yield about 2% MAC absolute error in neutral-point location.

Acknowledgment

This work was supported by the European Commission Research Directorates, Framework V, GROWTH Project GRD1-2000-25261.

References

[1]Kehlenbeck, U., "AIRBUS A340 Weight and Balance System," *The Proceedings of the 58th SAWE Annual Conference*, Society of Applied Weight Engineering (SAWE), Los Angeles, CA, 1999.

[2]Mack, R. J., "Rapid Empirical Method for Estimating the Gross Takeoff Weight of a High Speed Civil Transport," NASA TM-1999-209535, Oct. 1999.

[3]Funahashi, K., "On the Approximate Realization of Continuous Mappings by Neural Networks," *Neural Networks*, Vol. 2, No. 3, 1989, pp. 183–192.

[4]Demuth, H., and Beale, M., *Neural Network Toolbox for Use with MATLAB®—User Guide*, The MathWorks, Inc., Natick, MA, 2000.

[5]Cybenko, G., "Approximation by Superpositions of Sigmoidal Function," *Mathematics of Control, Signals, Systems*, Vol. 2, No. 4, 1989, pp. 303–314.

[6]Hornik, K., Stinchcombe, M., and White, H., "Multilayer Feedforward Networks Are Universal Approximators," *Neural Networks*, Vol. 2, No. 5, 1989, pp. 359–366.

[7]Haykin, S., *Neural Networks: A Comprehensive Foundation*, 2nd Ed., Prentice–Hall, Upper Saddle River, NJ, 1999.

[8]Morales, M. A., and Haas, D. J., "Feasibility of Aircraft Gross Weight Estimation Using Artificial Neural Networks," *The Proceedings of the 57th American Helicopter Society (AHS) International Annual Forum*, Alexandria, VA, 2001, pp. 1872–1880.

[9]"Project Program, Affordable Digital Fly-by-Wire Flight Control System for Small Commercial Aircraft—Second Phase (ADFCS-II)," Commission of the European Communities, Research Directorate, Framework V GROWTH Project GRD1-2000-25261, Brussels, Belgium, Sept. 2000.

[10]Ciniglio, U., "Synthetic Environment for Small Commercial Aircraft Simulation: User Manual," Centro Italiano Ricerche Aerospaziali, ADFCS-II Project Document ADFCSII/CIRA/T1.2/DOC/EML/19, Capua, Italy, June 2002.

[11]Etkin, B., and Reid, D., *Dynamics of Flight: Stability and Control*, 3rd Ed., Wiley, New York, 1996, p. 29.

[12]Raymer, D., *Aircraft Design: a Conceptual Approach*, AIAA Educational Series, AIAA, Washington, DC, 1991, p. 297.